DEVELOPMENT OF FINE STRUCTURAL DAMAGE TO ALVEOLAR AND CAPILLARY LINING CELLS IN OXYGEN-POISONED RAT LUNGS

GONZAGUE S. KISTLER, PETER R. B. CALDWELL, and
EWALD R. WEIBEL

From the Department of Anatomy, University of Zurich, Switzerland, and the 6570th Aerospace Medical Research Laboratories, Wright-Patterson Air Force Base, Ohio. Dr. Caldwell's present address is the Cardiopulmonary Laboratory, First Medical Division, Bellevue Hospital, New York. Dr. Weibel's present address is the Department of Anatomy, University of Berne, Switzerland

ABSTRACT

Rats were exposed to 98.5% oxygen at 765 torr for 6–72 hr. The pulmonary changes were investigated by electron microscopy and by morphometric methods. A progressive thickening of the air-blood barrier, from the normal 1.5 to 3 μ after 3 days, was due primarily to enlargement of the interstitial space by accumulation of edema which was replaced secondarily by cells and fibrin. This was accompanied by destruction of about 50% of the capillaries. Morphometric data allowed an estimate of the degree of impairment of lung function. The primary cellular damage was located in endothelial cells which underwent cytoplasmic changes and, finally, fragmentation. In contrast, the damage to the epithelial lining of alveoli was relatively scarce compared to the extensive endothelial changes. This pertained even to severely damaged lungs with 65% of the alveoli obliterated by a heterogeneous exudate. Possible causes for this apparently different reaction of epithelium (the first target cell) and endothelium to toxic oxygen effects are discussed.

INTRODUCTION

It is one of nature's puzzling paradoxes that oxygen, essential for the support of life, is toxic when breathed for prolonged periods at partial pressures higher than normal. The type of damage depends on the partial pressure prevailing: at a pO_2 around 1 atmosphere (atm) the respiratory system appears to react first, while at higher pressures the primary disturbances are noted in the central nervous system. The use of pure oxygen atmospheres in aviation, diving, and space travel, as well as the introduction of oxygen high pressure breathing into therapeutics recently has revived interest in the mechanisms of oxygen poisoning (1–8).

The present study was undertaken to elucidate the nature and time-course of damage occurring in the lungs of rats breathing essentially pure oxygen at atmospheric pressure. Previous studies (9–24) had shown that disturbances in the alveolar space and capillary bed (25) were associated with damages, in lung tissues, which comprise accumulation of edema fluid and cells in the interstitial space, a thickening of the air-blood barrier, and changes in the fine structure of cells (26–28). While these findings, for the most part, were recorded in terminal phases of oxygen poisoning, the present study attempts to define the time-course of events from their inception to their final stages, by apply-

ing methods of quantitative morphology and electron microscopy to a time series of oxygen exposure experiments.

In preliminary reports on this study (29, 30), emphasis has been placed on the functional aspects of damage to the lung as a gas exchange apparatus. The present report deals primarily with the cytological changes observed in the air-blood barrier, the tissue layer first exposed to the toxically elevated oxygen concentration.

MATERIAL AND METHODS

Experimental Animals

The present studies were conducted on young pure-bred male Sprague-Dawley rats born on the same day. 90 rats were divided into five groups; four test groups (1–4) which were sacrificed after 6, 24, 48, and 72 hr respectively, of exposure to a 98.5% oxygen atmosphere at 765 torr (Table I), and a control group (C) which was kept in room air until sacrifice under otherwise identical conditions.

Particular care was taken to eliminate from these groups all animals which showed any signs of murine pneumonia. Of the 90 rats, five thus had to be rejected (Table I).

Exposure to Oxygen

The test groups were brought simultaneously into an environmental chamber at the 6570th Aerospace Medical Research Laboratories, Wright-Patterson Air Force Base, Ohio. Technical design and facilities of this chamber have been described in detail elsewhere (31). A special study on a similar chamber (32) had failed to demonstrate the presence of any toxic contaminants under identical experimental conditions.

The chamber was supplied continuously with aviators' oxygen to maintain an average concentra-

TABLE I

Main Vital Characteristics of Rats Used

Group	Oxygen exposure	No. of animals	Age at sacrifice	Average body wt at sacrifice	No. of animals with murine pneumonia
	hr		days	gm SD	
C	—	14	44	123 ± 3	1
1	6	18	47	116 ± 1	2
2	24	17	48	119 ± 4	2
3	48	17	49	123 ± 4	0
4	72	24	50	102 ± 6	0

TABLE II

Characteristics of Chamber Atmosphere

Total ambient pressure, torr	765 (740 + 25)
Oxygen concentration, %	98.5 ± 1
Carbon dioxide concentration, %	Below 0.1
Relative humidity, %	46 ± 1
Temperature, °F	74 ± 2

± values: 1 standard deviation

tion of 98.5% oxygen throughout the experiments. It was pressurized 25 torr above ambient pressure, so that any possible leaks were outboard. The conditions prevailing in the chamber during the exposure period are shown in Table II.

Preparation of Lungs

At the end of exposure the animals of each group were anesthetized deeply by intraperitoneal injection of Nembutal (5 mg/100 g body weight), brought out of the chamber, weighed, labeled, and processed immediately in the following way: the trachea was exposed and opened, the chest was punctured to collapse the lungs, and a cannula was inserted into the tracheostomy. 2.5% glutaraldehyde, buffered to pH 7.4 with 0.03 M potassium phosphate, was instilled immediately at a standardized pressure of about 20 cm H_2O. The average time lapse between exit from the chamber and the start of instillation was 17 min, with a range from 4 to 35 min. After ligation of the trachea, the heart and lungs were removed en bloc from the chest and submerged in the fixative for 2 hr. Subsequently, heart and mediastinal tissue were dissected away carefully, and the lung volume was measured by fluid displacement.

Only lungs which were free of any signs of murine pneumonia and which were judged to be fixed perfectly were processed further. They were sliced with razor blades into alternately thick (3–5 mm) and thin (1 mm) slices.

The thick slices were embedded in celloidin-paraffin and prepared for light microscopy. The thin slices were cut into 200–300 small cubes of approximately 3 mm^3 which were washed for 2 hr in three changes of 0.11 M potassium phosphate buffer, postfixed for 90 min in buffered 1% OsO_4, dehydrated in ethanol, and embedded in Epon (33). From the total pool of cubes of each lung, a random sample of 20 pieces was embedded into consecutively numbered blocks; the remaining material was bulk-embedded in plates as reserve. Sections of 2–3 mm^2 area and 600–900 A thickness were cut with a diamond knife, and picked up on 150-mesh copper grids fitted with a carbon-reinforced Formvar film. Section contrast

TABLE III

Sample Size for Morphometry

| | No. per | | | Total No. |
	Field	Section	Animal	Group	
Animals				5	25
Sections			5	25	125
Micro-graphs		6	30	150	750
Test points	168	1008	5040	25,200	126,000

was enhanced with lead citrate (34). The electron micrographs were taken in a Philips EM 200.

Lungs fixed in glutaraldehyde followed by OsO_4 regularly show a granular contamination along cell membranes. So far, we have not been able to eliminate this contamination which does not occur in other tissues fixed the same way. Therefore, a smaller number of randomly chosen lungs of each group were instilled directly with buffered 1% OsO_4 to serve as technical controls; further processing remained unchanged.

Sampling of Material

The glutaraldehyde-fixed and processed lungs were numbered consecutively in order of time of fixation. For morphometric work the first five lungs were selected. Of each lung, again the first five blocks were sectioned. Random sampling of six fields per section for electron micrography was done according to methods previously described, placing the screen into one specified corner of the selected mesh of the copper grid (35, 36). The size of the sample obtained by this procedure is shown in Table III.

For descriptive study of cellular changes the same material was used. In addition, for each group a smaller number of sections from lungs directly fixed in OsO_4 also were investigated. Comparison of the two preparations revealed no essential differences in fine structural changes; all electron micrographs reproduced here have been taken from OsO_4-fixed material for purely aesthetic reasons.

Stereologic Methods

The electron micrographs used for morphometric study were recorded on 35 mm film. Contact prints of the negatives were analyzed in a table projector unit, the screen of which was fitted with a multipurpose test system comprising 84 lines and 168 test points (36). The stereologic methods allowing an estimation of surface areas, volumes, and average thicknesses of tissue layers have been presented previously in detail (35–37). The statistical signifi-

cance of the morphometric findings was tested by analysis of variance (38, 39).

RESULTS

General Observations

The first pathological changes were observed in animals removed from the chamber after 48 hr of breathing pure oxygen (group 3). They were dyspneic and, at autopsy, the normally pink and smooth lung surface was found to be mottled with small red and yellowish spots; the pleural cavity contained some exudate. These findings were exaggerated greatly in the last group of rats which remained in the oxygen atmosphere for 72 hr (group 4).

Light microscope preparations of the 6- and 24-hr groups (groups 1 and 2) revealed normal lung structure, while in group 3 a beginning formation of interstitial edema around some larger blood vessels could be observed. Lungs of group 4 showed striking changes in the alveolo-capillary region which were distributed focally over the whole lung: the interalveolar septa were thickened markedly and were rich in cells; alveoli were filled with a partly hemorrhagic exudate containing fibrin, numerous leukocytes, and macrophages. Morphometric analysis revealed that 65% of all alveoli were obliterated (29, 30), while about a third of the lung appeared normal in structure.

Morphometric Findings

Fig. 1 summarizes the essential morphometric findings which have been presented in detail else-
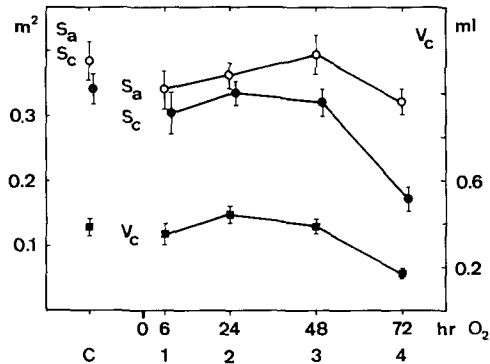

FIGURE 1 Alveolar surface area (S_a), capillary surface area (S_c), and capillary volume (V_c) in control rats (C) and during oxygen breathing for 6–72 hr. Brackets indicate standard errors of mean.

where (29, 30). The surface area of the alveolar epithelium (S_a) remained essentially unchanged throughout the entire experiment. The apparent reduction of S_a in group 4 was not found to be statistically significant.

In contrast, the capillary endothelial surface (S_c) and the capillary blood volume (V_c) fell, in group 4, to about 50% of their control values (p < 0.01), whereas no changes in these parameters could be detected at earlier time points. Comparison of Figs. 2 and 3 reveals that this can be explained by the destruction of capillaries within extended portions of interalveolar septa, accompanied by accumulation of leukocytes, fibrin strands, and cell debris in the tissue. In lungs of group 4, capillary blood occupied only 18% of the total septal volume as compared to 40% in the control lungs.

In the normal lung, the air-blood barrier, i.e. the tissue separating capillary blood from alveolar air, was estimated by a stereologic method to have an average thickness of 1.5 μ. As Fig. 4 shows, the average barrier thickness remained unchanged in groups 1 and 2, but increased to 2.1 and 2.9 μ in groups 3 and 4, respectively. It is evident from this diagram that this thickening is due essentially to a progressive enlargement of the interstitial space.

Normal Structure of Air-Blood Barrier

Since the structure of lung tissue in the normal rat has been described extensively in previous articles (40–43), only a few points essential for the present study shall be highlighted.

The tissue layers composing the barrier, capillary endothelium, alveolar epithelium, and interstitium are continuous throughout the lung (Fig. 2). The average thickness of the endothelium lining the capillary bed measures about 0.3 μ, that of the alveolar epithelium 0.65 μ, and that of the interstitium 0.55 μ (Fig. 4). From place to place, however, their thicknesses can vary considerably as is evidenced by Figs. 2 and 5–9.

The endothelial cells form broad extensions of 0.1–0.5 μ thickness (Figs. 5 and 8). In some regions these can be attenuated to 250 A whereby only an extremely thin layer of cytoplasm separates the two cell membranes (Fig. 9). However, no pores or fenestrae can be found in these lung capillaries (44, 45 a.o.). Organelles are concentrated in the thicker perikaryon; the extensions contain only scarce and small mitochondria, scattered profiles of endoplasmic reticulum, and a few ribosomes. Micropinocytotic vesicles are numerous in all

Key to Symbols

A, alveolar space
BM, basement membrane
C, capillary lumen
CF, collagenous fibrils
EC, erythrocyte
ED, edema fluid
EF, elastic fibers
EN, endothelium
EP, epithelium
ER, endoplasmic reticulum
FB, fibroblast
FF, fine filaments
FI, fibrin

GO, Golgi vesicles
GS, ground substance space
IN, interstitium
J, intercellular junction
LC, leukocyte
LD, lipid droplet
MA, macrophage
MI, mitochondrion
MV, microvilli
N, nucleus
OL, osmiophilic lamellated bodies
T, thrombocyte
TM, tubular myelin figures

FIGURE 2 Normal interalveolar septum of control rat lung. Thick parts of air-blood barrier contain interstitial elements and cell bodies of endothelial and epithelial cells while thin barrier portions are formed by slim cytoplasmic extensions of epithelium and endothelium separated by fused basement membranes. X 5,900.

FIGURE 3 Interalveolar septum of rat lung after 72 hr exposure to oxygen. Note destruction of capillaries (C') and remnants of endothelium, as well as leukocyte in interstitium. Tubular myelin figure in alveolar space. X 10,000.
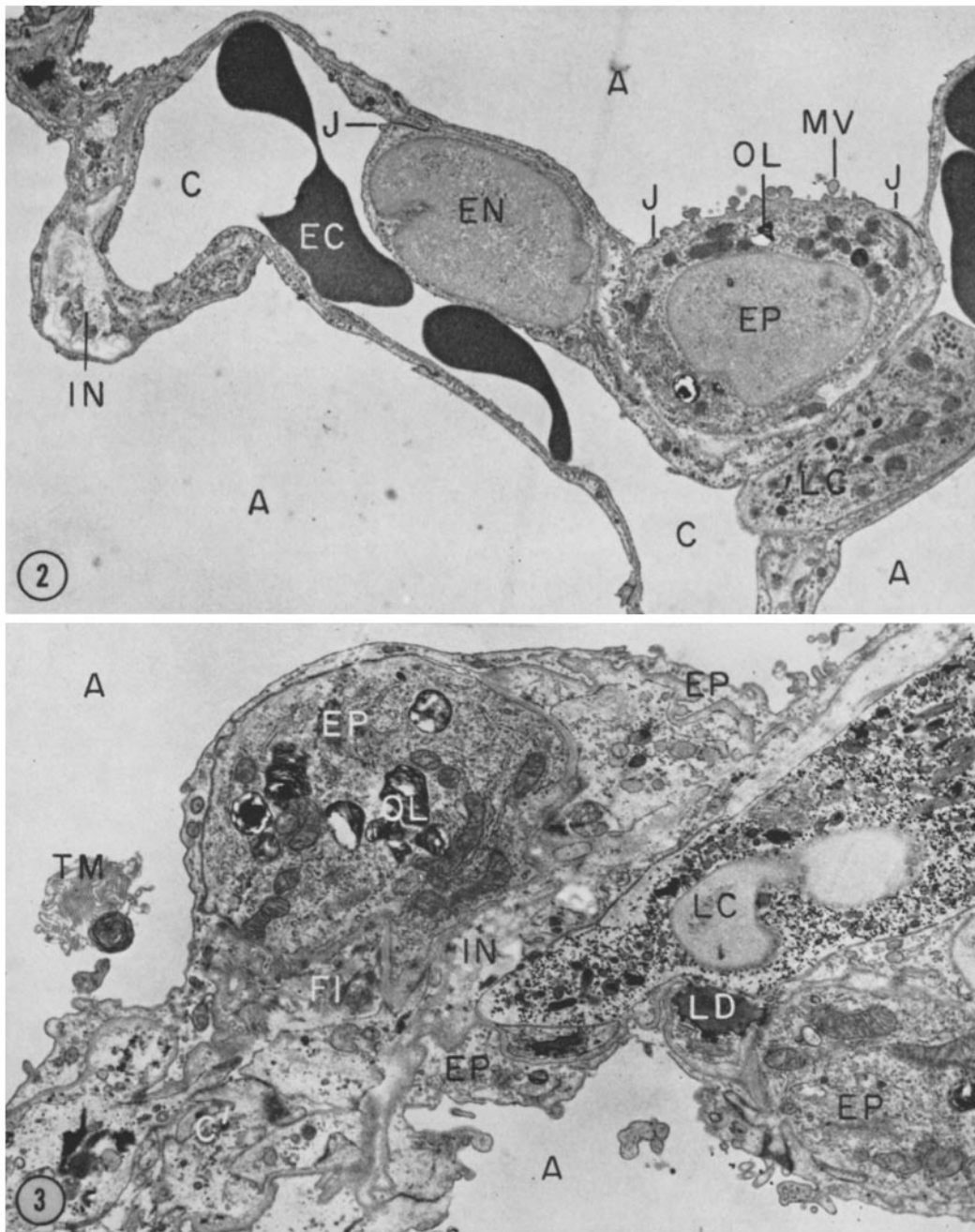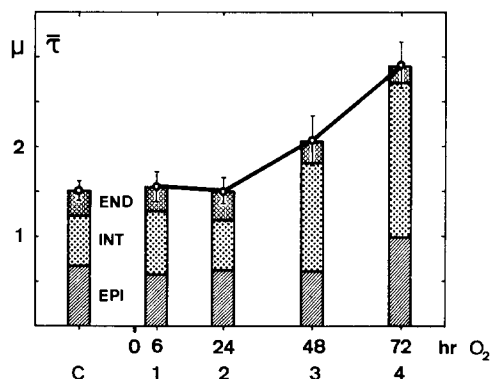
FIGURE 4 Change in average thickness $\bar{\tau}$ of air-blood barrier and of its composition in terms of endothelium (END), interstitium (INT), and epithelium (EPI). Brackets are standard errors of mean.

parts. The extremely attenuated portions (<1000 A) are entirely free of organelles (Figs. 8 and 9). At intercellular junctions the plasma membranes become closely apposed to each other in the luminal half of the contact zone (Figs. 5-8). As shown in Figs. 6 and 7 the gap between the osmiophilic layers is less than 100 A; there is a suggestion of a faint intermediate line, so that these appear to be zonulae occludentes (46). In their immediate vicinity the density of cytoplasm is increased slightly (Fig. 7).

The alveolar epithelium is composed of two cell types. The so-called small or type I alveolar cells are similar to endothelial cells with broad and thin extensions, and form the major part of the alveolar lining (Fig. 2). The distribution of cytoplasmic organelles and the structure of intercellular junctions correspond to that described above for endothelial cells (Figs. 5 and 8). The large alveolar epithelial cells (type II) have no extensions, but contain the characteristic, lamellated, osmiophilic granules (Figs. 2 and 24), (42, 47). Towards the alveolar lumen these cells form numerous, short

microvilli. The junctions between large and small epithelial cells also contain a zonula occludens (Figs. 2 and 26).

The basement membranes of the epithelium and endothelium delimit the interstitium, which in some parts is reduced so far that the two basement membranes appear fused (Figs. 5, 6 and 9). In other parts the interstitial space is wider and contains fibroblasts, elastic fibers, and slim bundles of collagenous fibrils (Fig. 8). Some fine interstitial filaments are associated primarily with elastic fibers (Fig. 8). In view of the present study it is important to emphasize that the ground substance space of the pulmonary interstitium is very narrow in all parts of the air-blood barrier.

Structural Changes Observed after Oxygen Exposure

INTERSTITIUM: Fig. 4 indicates that the first changes in fine structure of the air-blood barrier become evident after 48 hr of oxygen breathing; they are recorded as an enlargement of the interstitial space from the normal 0.55 to 1.2 μ (Fig. 10). This thickening is statistically highly significant (P < 0.01) but earlier variations in thickness (group 1) are not significant. The widening of the interstitial space progresses during the third day of exposure to 1.7 μ on the average, i.e., to triple of control value.

A comparison of Fig. 11 with Figs. 2, 5, and 8 immediately reveals that in lungs of group 3, fluid has accumulated in the ground substance space of the interstitium. Epithelial and endothelial basement membranes, fibroblasts, and formed interstitial elements are separated by wide, empty spaces. The portions of the barrier in which epithelial and endothelial basement membranes are fused (Figs. 5 and 6) do not imbibe edema fluid (Fig. 11). 24 hr later, a peculiar granularity often appears over wide, edema fluid-filled spaces (Fig. 12). In other regions of group 4 lungs, numerous

FIGURE 5 Air-blood barrier of control rat lung with narrow interstitium. Note fusion of basement membranes (BM') in thinnest portions. × 47,100.

FIGURE 6 Higher magnification of intercellular junction of endothelium in Fig. 5. Note close apposition of cell membranes in luminal half. × 85,600.

FIGURE 7 Demonstration of zonula occludens in junction of capillary endothelial cells. Note intermediate line (arrow) and condensation of cytoplasm near junction. Uranyl acetate and lead stain. × 186,000.
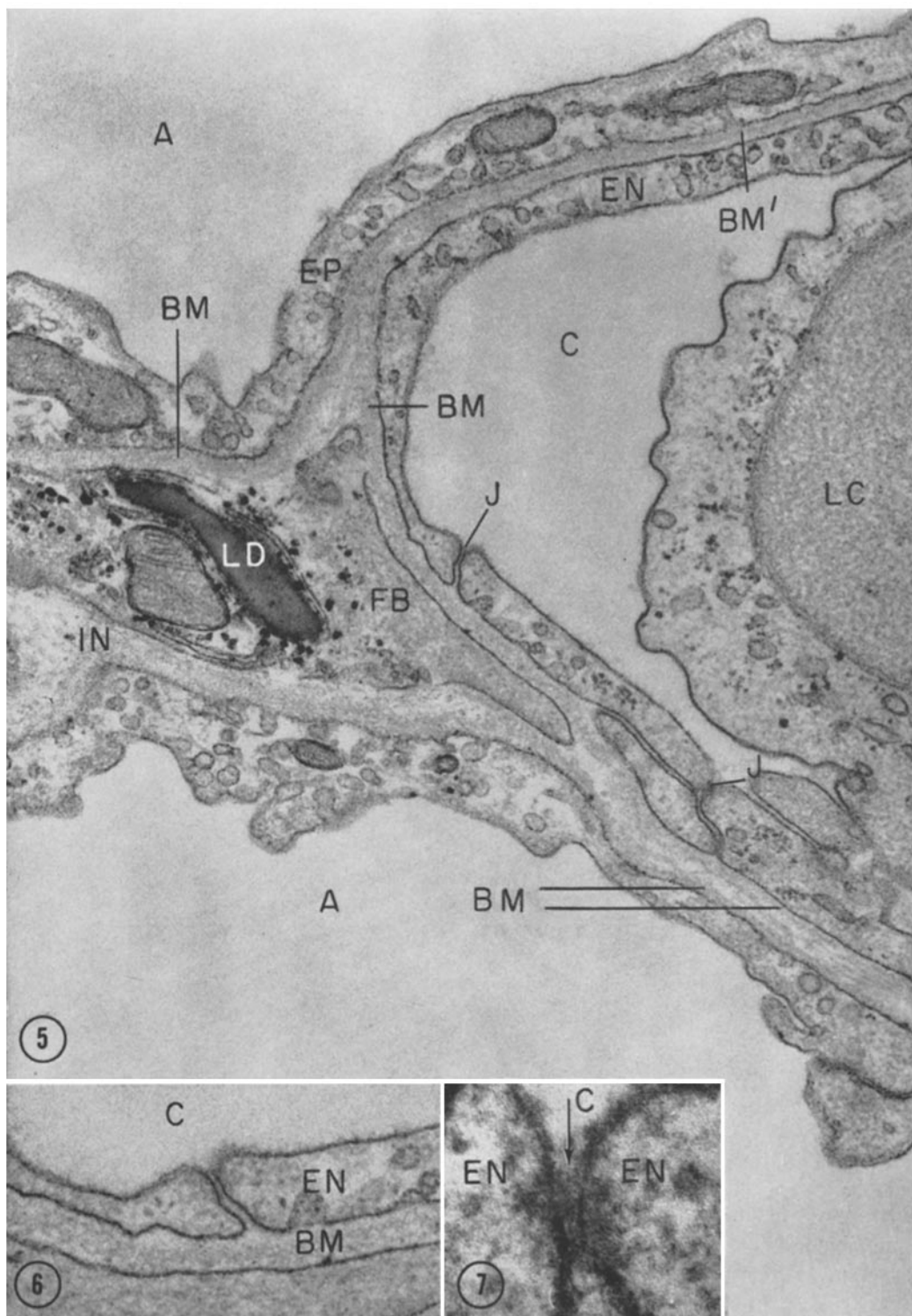
FIGURE 8 Thick part of air-blood barrier containing the various, formed elements of interstitium between endothelial and epithelial linings. × 57,800.

FIGURE 9 Extremely attenuated portion of endothelium. Note complete absence of organelles and single (fused) basement membrane between epithelium and endothelium. × 57,800.

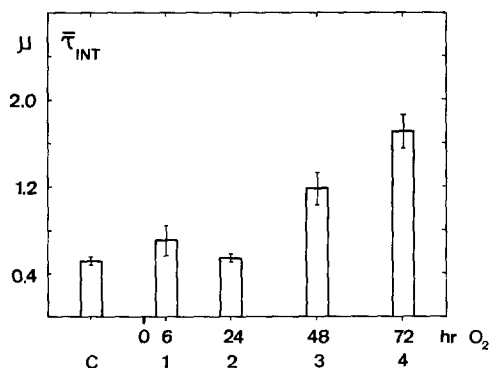μ | $\bar{\tau}_{INT}$

2.0

1.2

0.4

    0 6   24   48   72 hr O_2
    C   2   3   4
    1

FIGURE 10 Change in average thickness of interstitial space. Brackets are standard errors of mean.

The lumen of this capillary contains thrombocytes and cell debris which is probably fragments of destroyed endothelial cells. Such fragments are also apparent on Fig. 17.

Fig. 20 reveals the varying picture of endothelial cell necrosis. Two profiles appear as empty, markedly swollen membrane sacs void of organelles; in others the cytoplasm is condensed and fragmented partially. Tight intercellular junctions can be recognized no longer. The endothelial basement membrane, however, is still intact. The capillary lumen contains no blood plasma. The hemoglobin of some red cell fragments is leached out partly.

Figs. 21 and 22 illustrate the final stage of endothelial cell destruction. The capillary is bounded exclusively by its basement membrane which is in direct contact with erythrocytes. Blood plasma is lacking and fibrin strands appear near the basement membrane.

EPITHELIUM: In spite of the drastic destruction of endothelial cells, the alveolar epithelium shows little change (Figs. 3, 18, 20–22). Even in group 4 the fine structure of the cytoplasm and organelles of the vast majority of small epithelial cells appears normal; interalveolar septa which contain only destroyed capillaries still may be covered by a seemingly intact epithelial lining (Figs. 21 and 22). In some rare areas, however, the entire barrier appears torn (Fig. 23), so that a continuity is established between blood vessels, interstitium, and alveolar space. Here it often can be observed that fibrin masses extend from the tissue space into exudate-filled alveoli.

The majority of large alveolar epithelial cells again shows normal fine structure even after 72 hr of oxygen exposure (Fig. 24). In some of these cells, however, a swelling of all membrane-bounded organelles, i.e. mitochondria, endoplasmic reticulum, perinuclear cisternae, and Golgi vesicles, is observed whereas the cytoplasmic ground substance is unaltered and is still rich in ribosomes (Fig. 25). In other instances the additional rarefaction of cytoplasmic ground substance appears to be due to imbibition of fluid (Fig. 26). The occurrence of cellular debris in alveoli after 72 hr (Fig. 20) suggests that such cells eventually may be destroyed.

Two-thirds of the alveoli of group 4 lungs were obliterated by a heterogeneous exudate which contained fibrin strands, cell debris (Fig. 20), and a peculiar myelin material (Figs. 3, 11, 27 and 28) which has been described in detail elsewhere (48).

leukocytes and thrombocytes appear to have migrated into the interstitium (Figs. 3 and 13), and parts of the ground substance space contain fibrin strands (Figs. 21 and 23). Interstitial macrophages appear there and cell debris from destroyed blood vessels is present.

ENDOTHELIUM: The appearance of interstitial edema after 2 days of oxygen breathing suggests damage to endothelial cells. Morphometrically a statistically significant reduction of the average thickness of endothelium is detectable only after 3 days (Fig. 14).

Close examination of endothelial cells in groups 1 and 2 did not reveal any structural changes. In group 3 the vast majority of endothelial cells appeared entirely normal in structure, even in highly edematous areas of the barrier; in particular, the cell junctions were tight (Figs. 11, and 15). Peculiar changes occurred in scattered marginal regions of endothelial cells: the cytoplasm adjacent to intercellular junctions appeared slightly swollen, of often homogeneously increased density, and void of organelles (Fig. 16 and 17), while the junctions themselves were accentuated by augmented contrast (Fig. 17). These alterations in marginal cell structure also could be observed in group 4.

After 3 days of oxygen breathing, a large fraction of endothelial cells showed drastic changes. In Fig. 18 one of the cells lining the capillary is characterized by strikingly dark cytoplasm in which mitochondria, endoplasmic reticulum, ribosomes, and Golgi vesicles still can be recognized (Fig. 19). The junction with the adjacent cell is still tight; however, this obviously damaged cell is detached partially from its basement membrane.
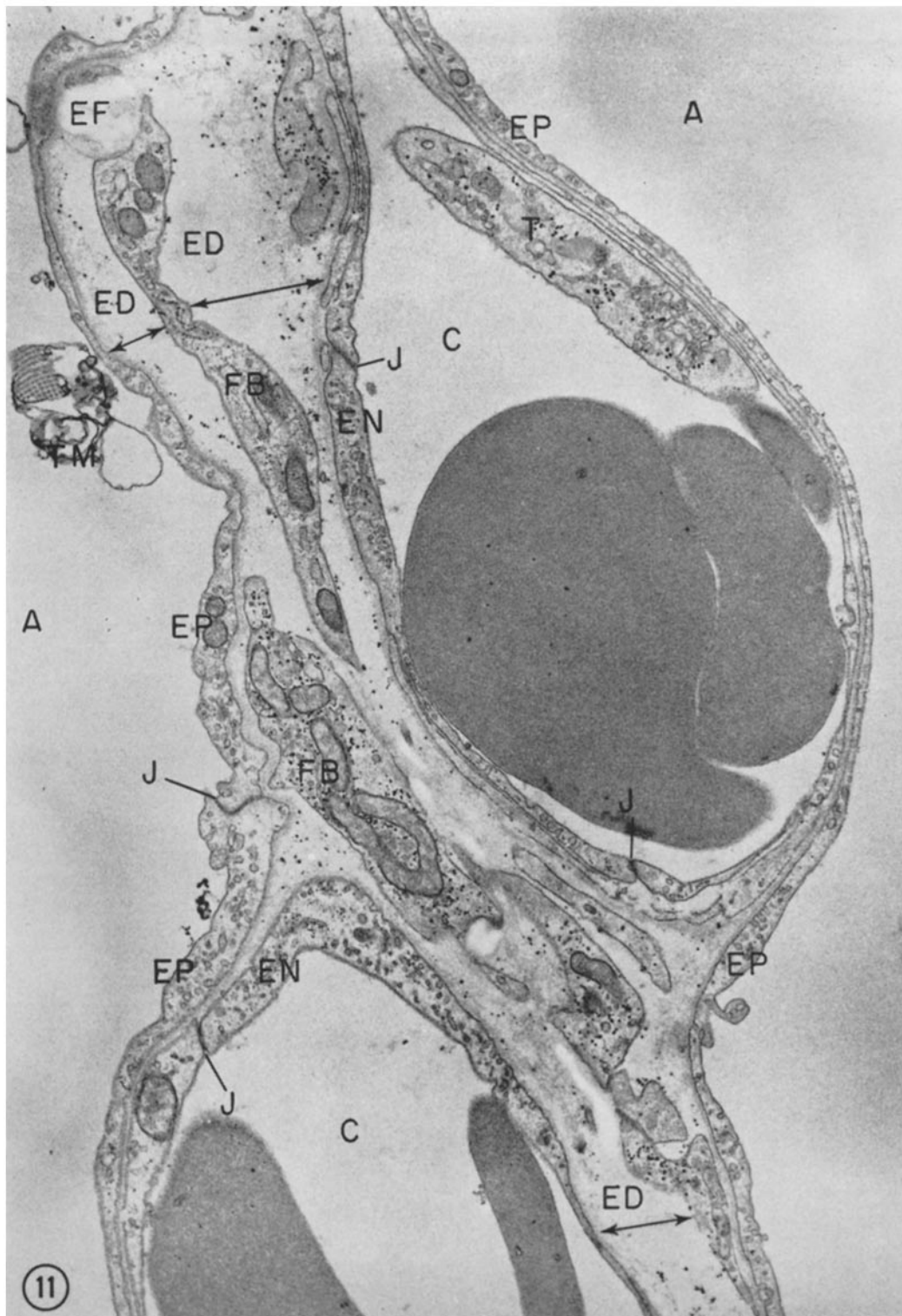
FIGURE 11   Interalveolar septum after 48 hr of oxygen breathing. Note enlargement of ground substance space of interstitium by edema (*ED*). Compare with Figs. 2, 5, and 8. Alveolar and capillary linings apparently unchanged. × 18,300.

This material consists of spheroid bodies of concentrically arranged osmiophilic lamellae, possibly phospholipid in nature (48), which are associated with highly ordered structures. These exhibit a fingerprint-like pattern on section; stereologic analysis has shown that they are composed of densely, packed, square tubules of 450 A diameter that contain a fine inner tubule of 250 A. In some instances the inner tubule may be replaced by a thin central filament (Fig. 28), in which case the tubule diameter is 380 A (48). It should be noted that this material also is found in small quantities

in normal lungs of many species (48–50), but never in masses as large as those observed here.

Besides leukocytes and erythrocytes, macrophages were numerous in the alveolar exudate; in Fig. 27 a macrophage is shown in the process of phagocytosing myelin material.

DISCUSSION

Time Sequence of Pathological Changes

The first changes detectable in lung tissue appear to develop during the second day of pure
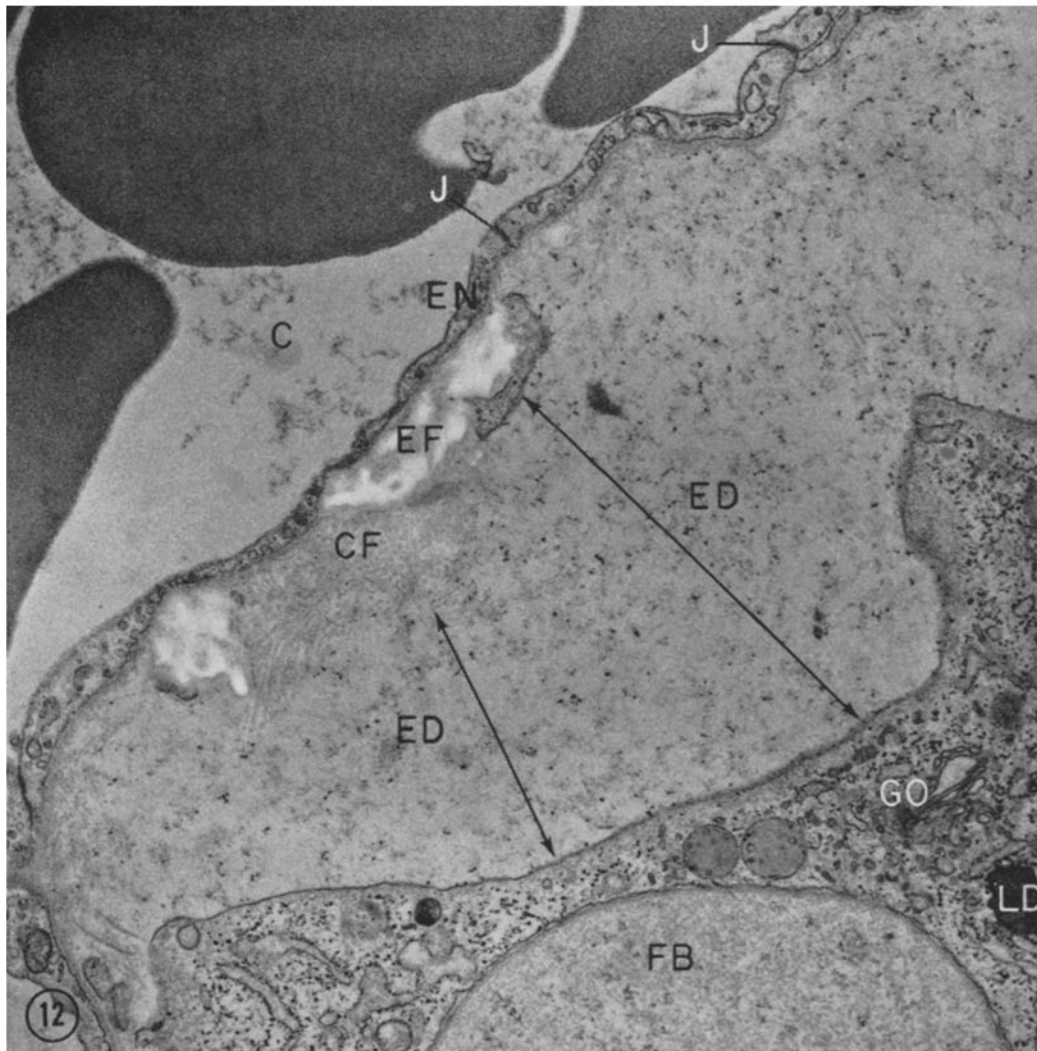

FIGURE 12 Edematous enlargement of interstitial ground substance space after 72 hr exposure to oxygen. Connective tissue fibers are separated from fibroblast by edema fluid showing granular precipitate of unknown nature. × 18 500.
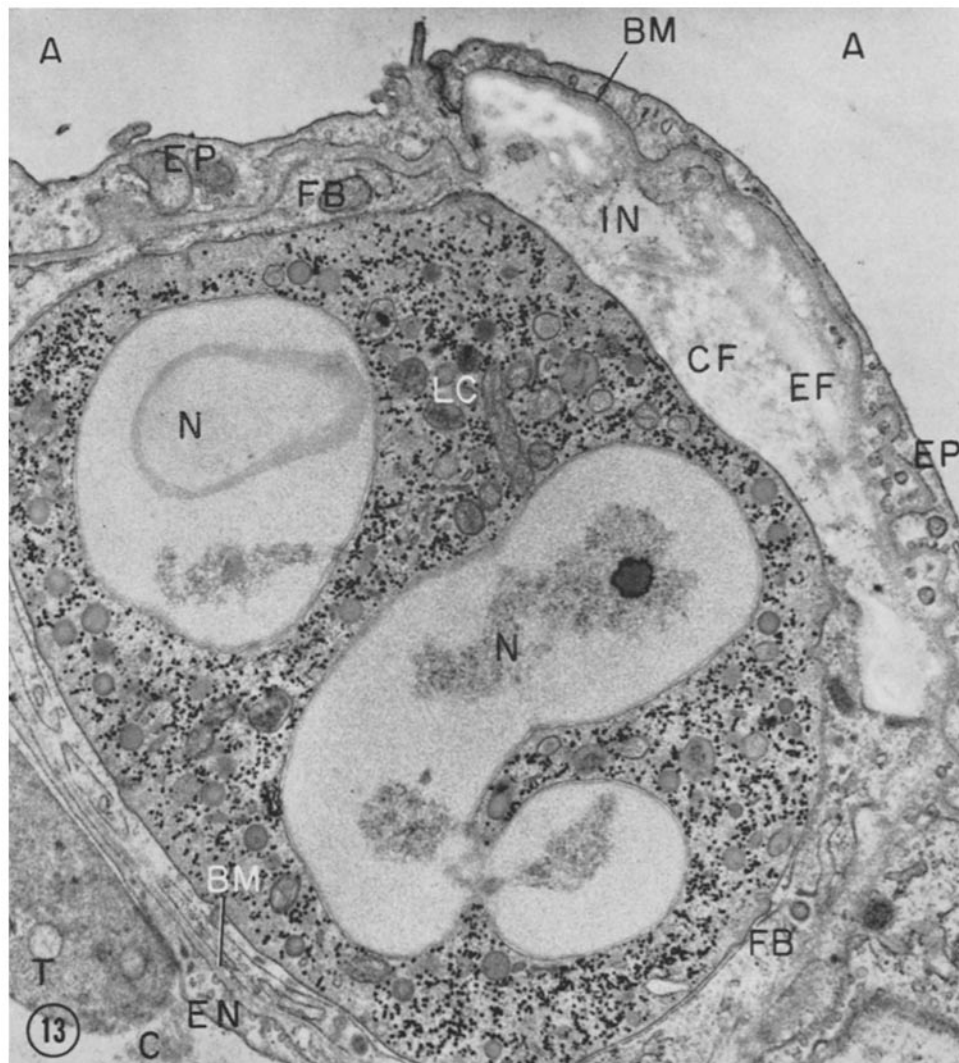
FIGURE 13   Neutrophil granulocyte in interstitium of interalveolar septum after 72 hr exposure to oxygen. Epithelium and endothelium intact. × 21,800.
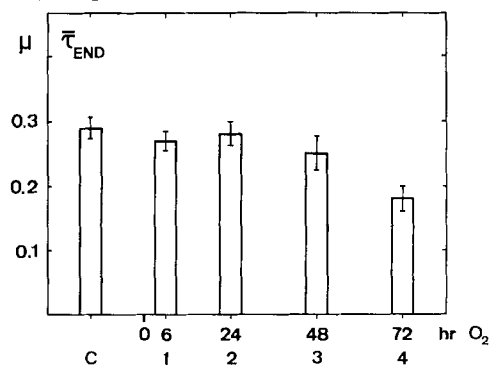

FIGURE 14   Changes in average thickness of endothelium. Brackets are standard errors of mean.

oxygen breathing and consist of edematous imbibition of the interstitial space. In light microscope preparations this is noted in the connective tissue sheath around some larger blood vessels. Electron microscopy revealed a progressive edematous enlargement of the normally slim interstitium of the alveolo-capillary air-blood barrier. It must be assumed, therefore, that the permeability of the capillary lining is increased, although only very minute and inconspicuous changes in fine structure of endothelial cells can be recognized at this stage.

During the third day a structural damage to endothelial cells develops, which results in complete destruction of the lining of a large fraction of
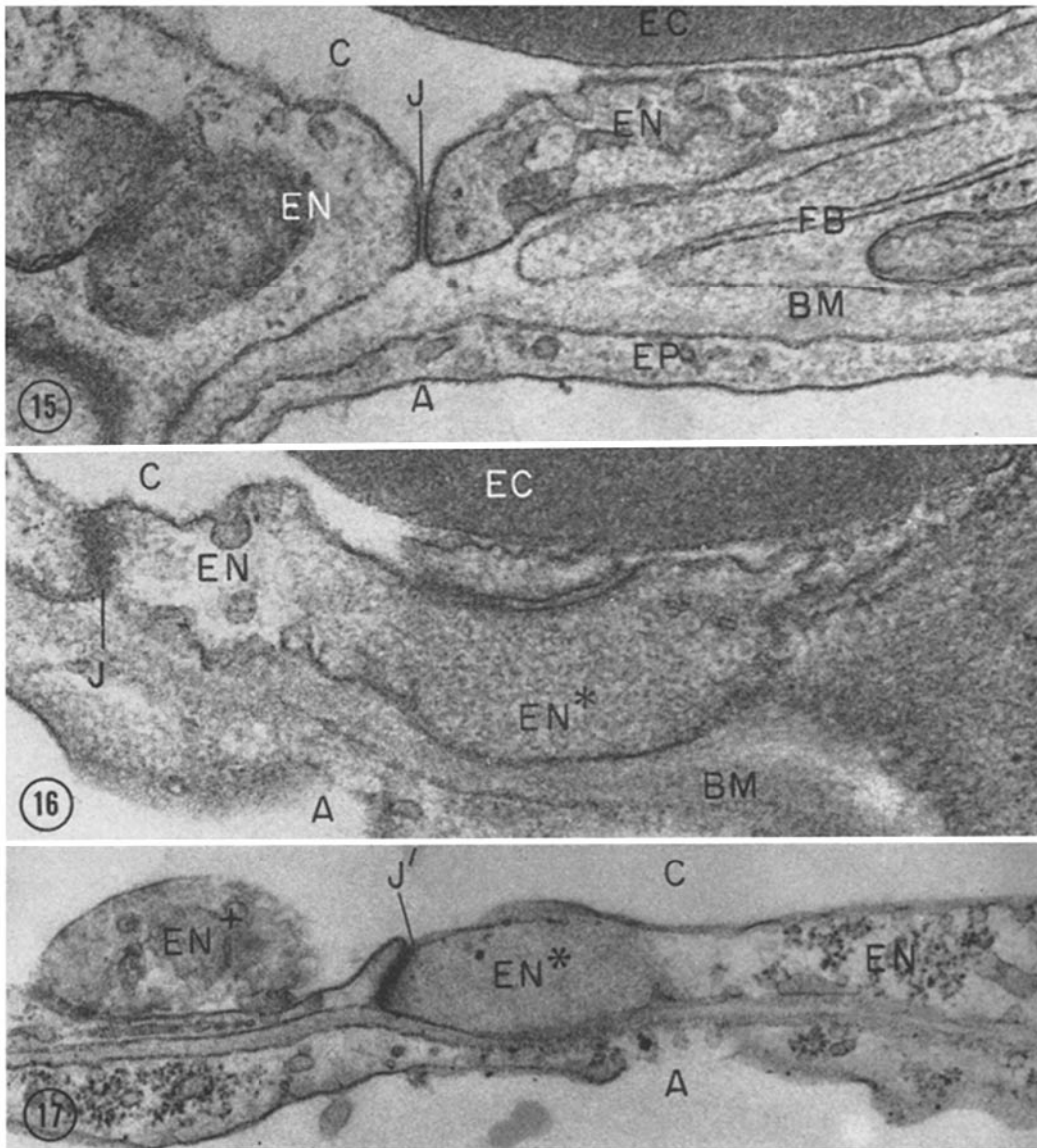
FIGURES 15–17 Marginal changes in endothelial cells after 48 hr exposure to oxygen.

FIGURE 15 Endothelium and junction apparently unchanged. × 69,900.

FIGURE 16 Granular condensation of marginal cytoplasm (EN*); junctions unchanged. × 80,400.

FIGURE 17 Granular condensation and bulblike swelling of marginal cytoplasm free of organelles (EN*) next to apparently normal cytoplasmic structure (EN). Capillary lumen contains cell debris of probably endothelial origin (EN+). Contrast of intercellular junction (J') accentuated. × 43,700.

the capillaries. This causes the capillary volume, as well as the capillary surface area, to fall to about 50% of the control values. Concurrently, leukocytes, macrophages, and thrombocytes, as well as fibrin strands, appear in the edematous interstitium. During the third day profuse exudation of a plasma-like fluid containing fibrin and numerous free cells obliterates up to two-thirds of the alveoli. This is accompanied by remarkably little damage to alveolar epithelium. In contrast to the massive destruction of capillary endothelium, the vast majority of epithelial cells show normal fine structure.

Progressive Impairment of Lung Function

The edematous thickening of the alveolo-capillary air-blood barrier, the loss of capillaries, and the obliteration of alveoli lead to an impairment of pulmonary gas exchange. In our experiments, this resulted in marked dyspnea, cyanosis, and asphyxia of the animals when these were brought back to room air after 3 days of pure oxygen breathing. This finding is consistent with observations made on other mammals and on man (9, 12, 15–18, 24, a.o.).

At earlier time points the animals showed no signs of asphyxia upon removal from the pure oxygen atmosphere. Nonetheless, pulmonary gas exchange must have been impaired already at the end of the second exposure day; calculation of a model value for the diffusing capacity of the barrier, from morphometric data, revealed that this parameter fell to 83% of the control value. During the third day the diffusing capacity thus estimated was reduced further to 25% (29, 30). The obliteration of two-thirds of the alveoli by edema fluid added to this functional damage; it was estimated that only some 10% of the original capacity of the lung for gas exchange remained available at this terminal stage. In experiments on human volunteers under equivalent conditions, Caldwell et al.

(32) recorded a fall in pulmonary diffusing capacity to 81% of the control value after 48 hr and to 73% after 74 hr. Thus the measured drop in diffusing capacity in humans breathing pure oxygen correlates closely with the presently predicted fall in diffusing capacity of rats exposed to the same conditions. The fall in total lung capacity observed by these authors correlates with the obliteration of terminal air spaces by edema in our experiments.

Nature of Fine-Structural Changes

Most investigators agree that formation of interstitial and alveolar edema is a consistent finding in pulmonary pathology of severe oxygen poisoning (4, 10, 12, 15–17 a.o). This study has shown that interstitial edema of the pulmonary air-blood barrier develops while the architecture and fine structure of the lung seemingly are unchanged, and before any toxic effects on the organism become apparent.

This edema could form as a direct toxic effect of oxygen on some constituent of interstitial tissue, resulting in elevated osmotic pressure and swelling of the ground substance. Or, it may be the consequence of a primary vascular damage, for which two mechanisms can be imagined: (a) generalized spasm of small blood vessels, as found in the retina under the influence of oxygen breathing (51–53 a.o.), could cause elevated intracapillary pressure and movement of fluid into the tissue; (b) increased capillary permeability may be the result of direct injury to the endothelium.

While none of these possible causes can be excluded, the evidence presented in this study points to a local damage to endothelial cells as the primary cause for displacement of fluid, and eventually of cells, into the interstitium. In initial stages of edema formation, the endothelial lining of alveolar capillaries appears to be morphologically intact; the intercellular junctions are tight.

FIGURE 18 Alveolar capillary after 72 hr exposure to oxygen. Cytoplasm of one endothelial cell (EN^*) shows very marked electron-density; its junction with apparently unaltered neighboring cell (EN^0) seems intact. Note slight detachment from basement membrane (ED'). Capillary lumen contains thrombocytes (T) and cell debris of probably endothelial origin (EN^+). Alveolar macrophage (MA') adjacent to unchanged alveolar epithelium (EP). $\times$ 15,800.

FIGURE 19 Higher magnification of "dark" endothelial cell in Fig. 18. Organelles are embedded in finely granular, dense cytoplasmic ground substance. Note edematous bleb (ED') between cell and basement membrane. $\times$ 46,700.
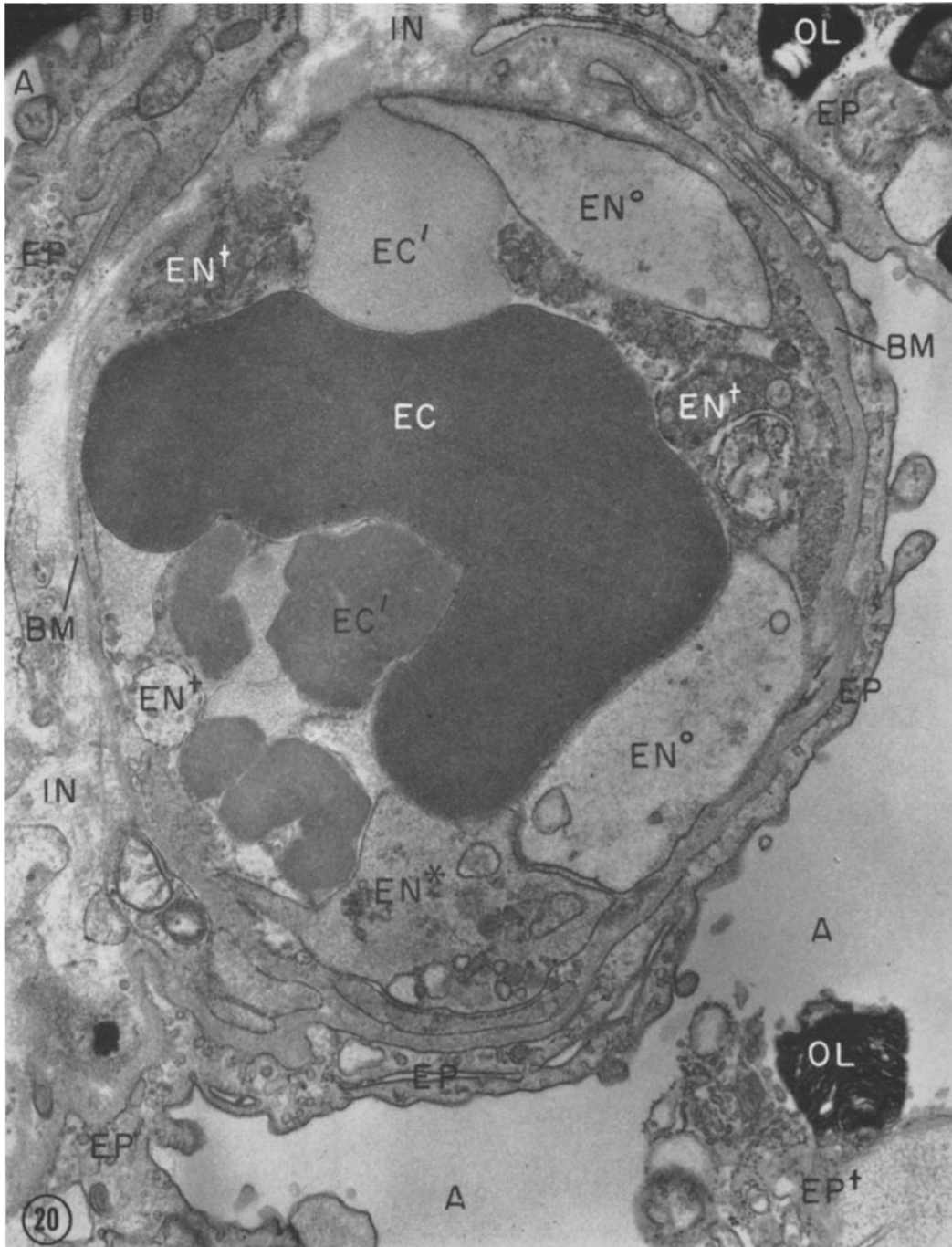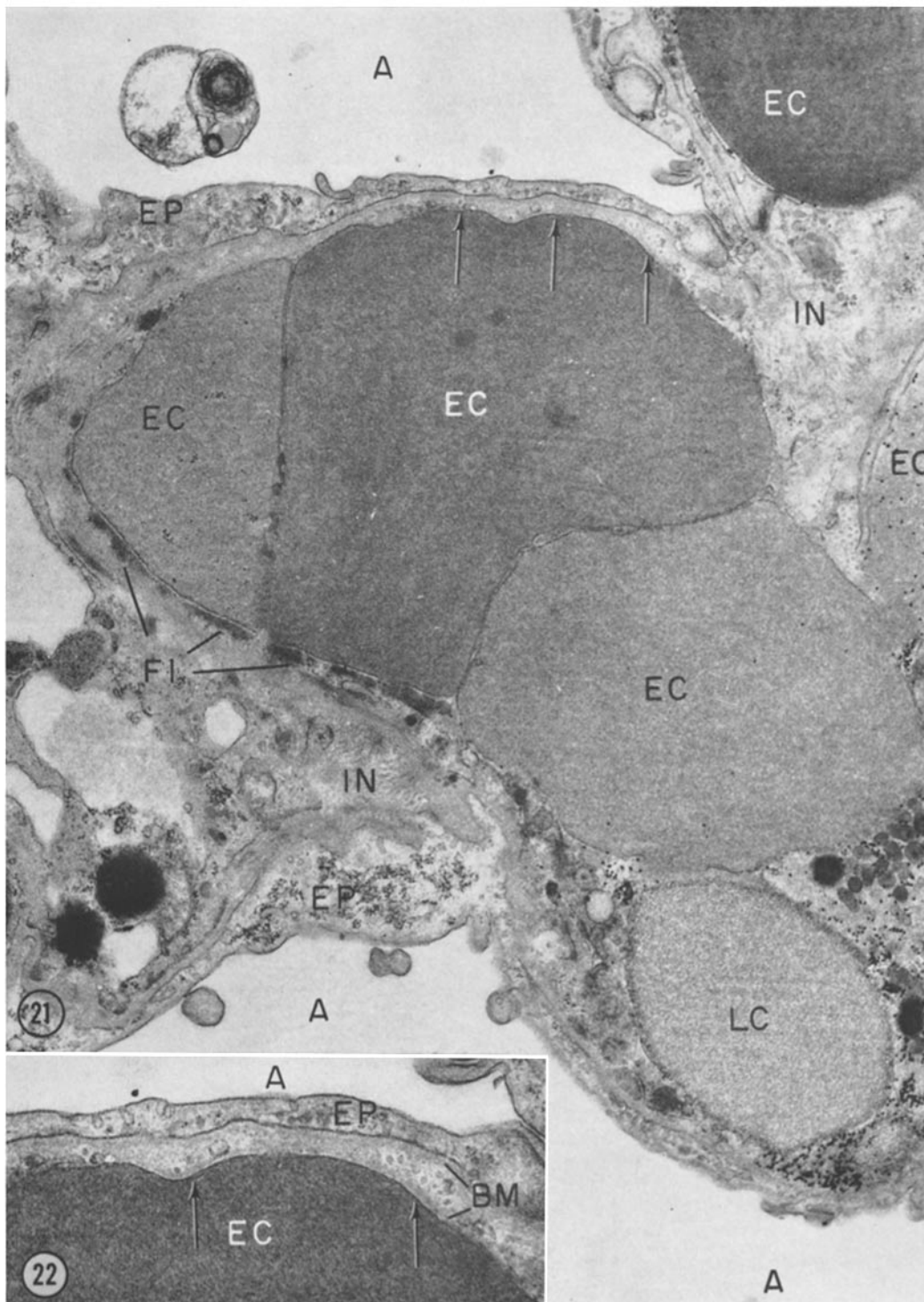
FIGURE 20   Alveolar capillary after 72 hr of oxygen breathing, showing different pictures of endothelial cell destruction: swollen cytoplasm free of organelles (EN^0), condensation of cytoplasm (EN^*), and fragmentation of cells (EN^+). Basement membrane is preserved. Epithelial lining still intact and of apparently normal fine structure. Alveolus contains cell debris of large alveolar epithelial cell (EP^+) with osmiophilic lamellated body (OL). Capillary lumen contains one seemingly normal red cell (EC) and various erythrocyte fragments (EC') of varying electron-density. $\times$ 26,600.

FIGURES 21 and 22   Alveolar capillary after 72 hr exposure to oxygen has lost its endothelium. Tightly packed erythrocytes in former lumen are in direct contact with endothelial basement membrane (arrows), as is clearly shown at higher magnification in Fig. 22. Fine fibrin strands (*FI*) appear near basement membrane. Epithelial lining of alveolus intact. Fig. 21, × 16,500; Fig. 22, × 33,900.

Sparse marginal regions of endothelial cells show a peculiar change in cytoplasmic fine structure: a loss of organelles is accompanied, in part, by swelling and, in part, by granular condensation of cytoplasmic ground substance. This appears to initiate, during the 3rd day of oxygen breathing, the progressive destruction of endothelial cells which manifests itself in either swelling or granular condensation of cytoplasm followed by fragmentation. Previous cytological studies of oxygen effect on the lung (26, 27) have not emphasized

this primary endothelial damage, although Cedergren et al. (28) mention vacuolar swelling of endothelial as well as epithelial cells. In our study, alveolar epithelial cells of both types showed remarkably few cytological changes even in regions with complete destruction of capillaries. Occasionally, swelling of mitochondria and cisternae of endoplasmic reticulum was observed in some epithelial cells of the large type. This well may be a secondary injury due to the heavy damage of surrounding tissues. Cytological changes described
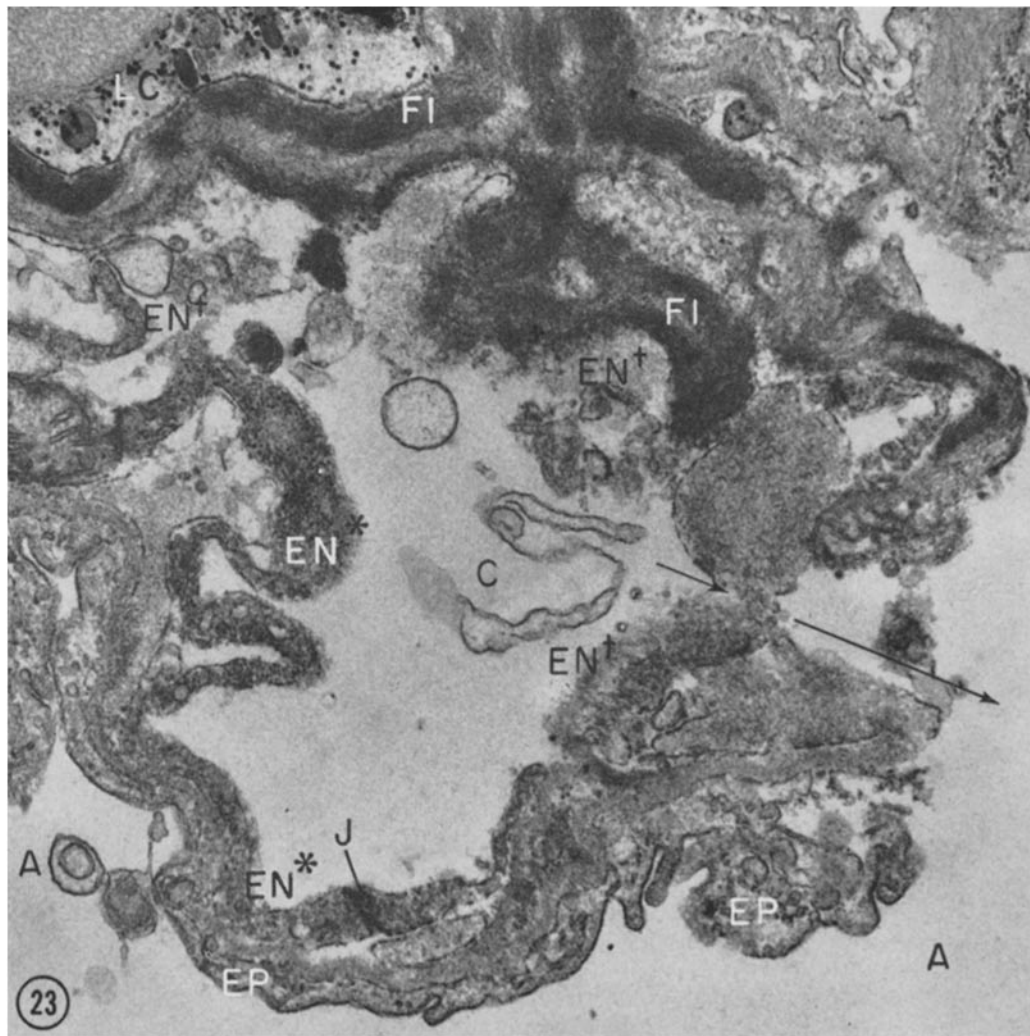

FIGURE 23 Disruption of air-blood barrier (arrows) in alveolar capillary after 72 hr of oxygen breathing. Condensed remnants of endothelial lining (EN*) and fragmented cells (EN⁺) mark former capillary lumen. Note fibrin strands (FI) in capillary lumen and interstitium. × 32,600.
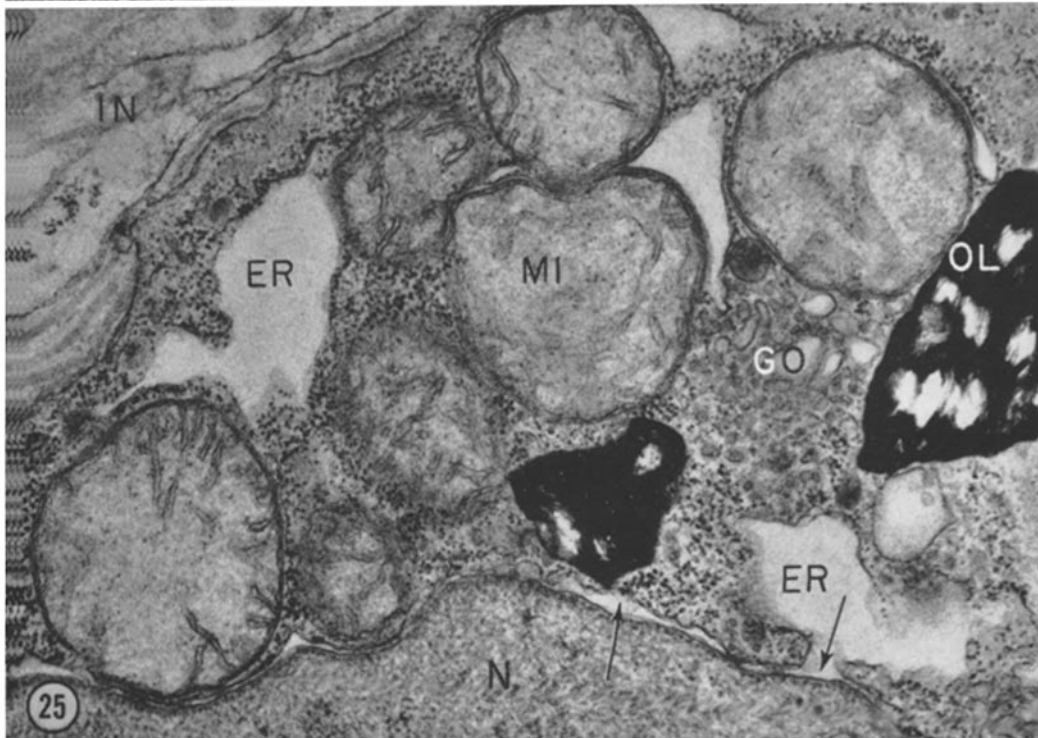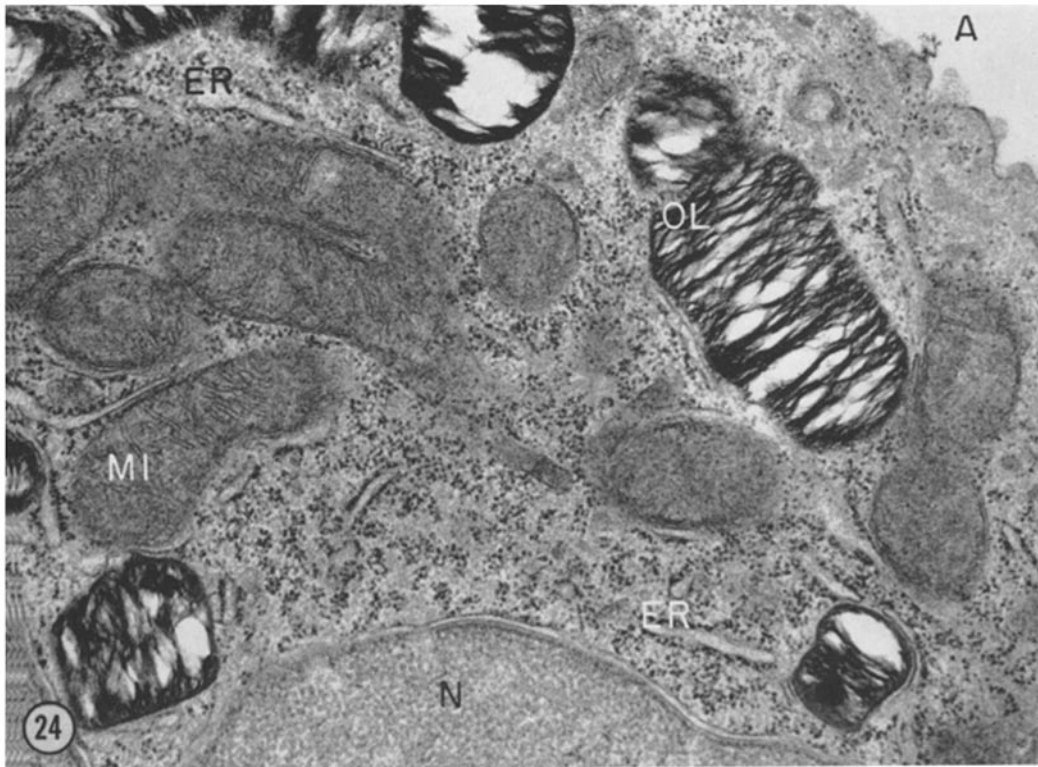
FIGURE 24   Large alveolar epithelial cell with osmiophilic lamellated bodies after 72 hr exposure to oxygen. Normal appearance of cytoplasmic structures. × 34,000.

FIGURE 25   Large alveolar epithelial cell from same lung as Fig. 24. Note swelling of mitochondrial matrix, of cisternae of endoplasmic reticulum continuing into perinuclear cisterna (arrows), and of some Golgi vesicles. Ribosome content of cytoplasmic ground substance unchanged. × 34,000.
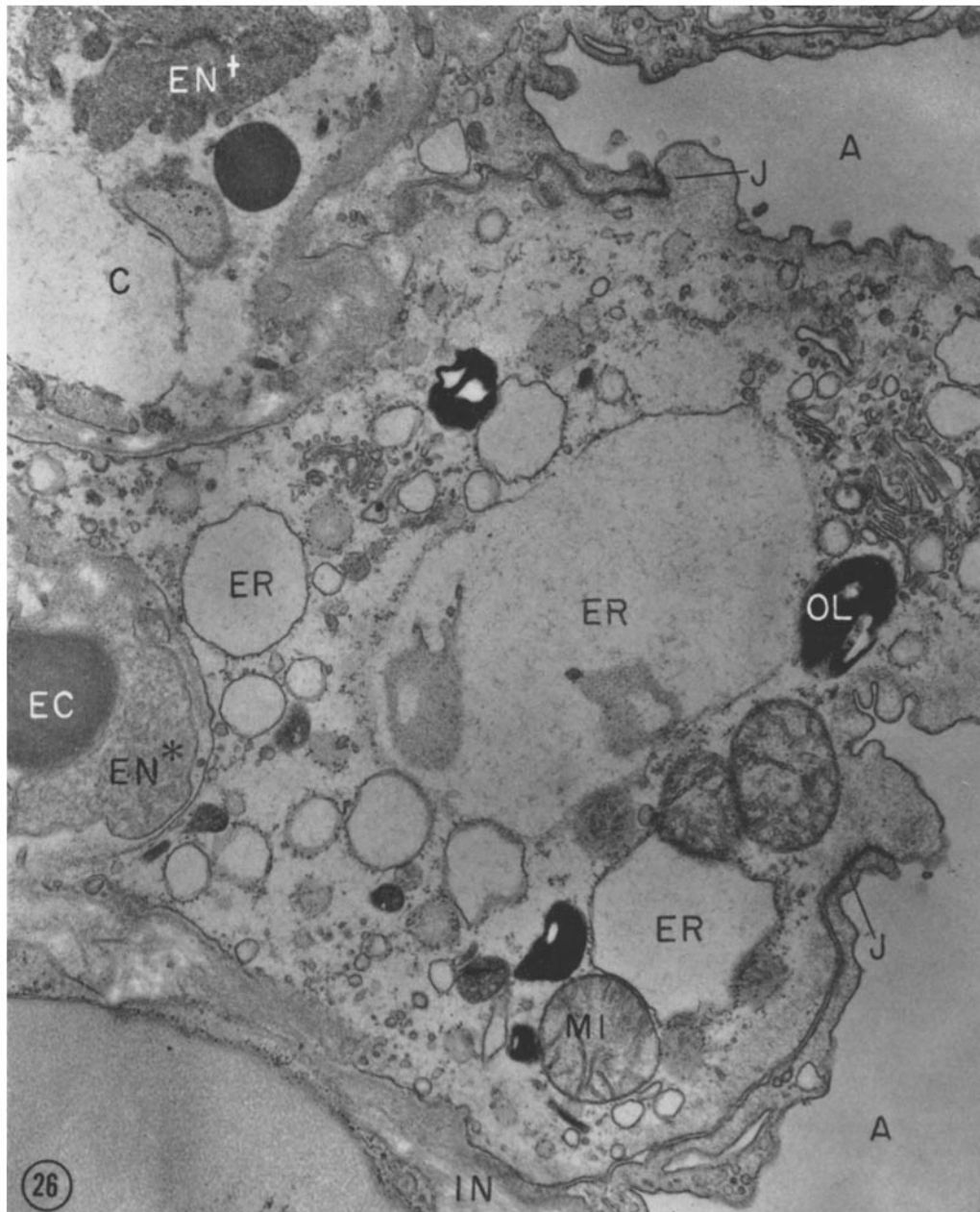
FIGURE 26   Large alveolar epithelial cell after 72 hr exposure to oxygen. Pronounced swelling of membrane-bounded organelles, particularly of cisternae of endoplasmic reticulum (*ER*). Major part of cytoplasmic ground substance exhibits edematous imbibition. Cell membrane and intercellular junctions are intact. Note destroyed capillary endothelium (*EN** and *EN+*). × 21,800.
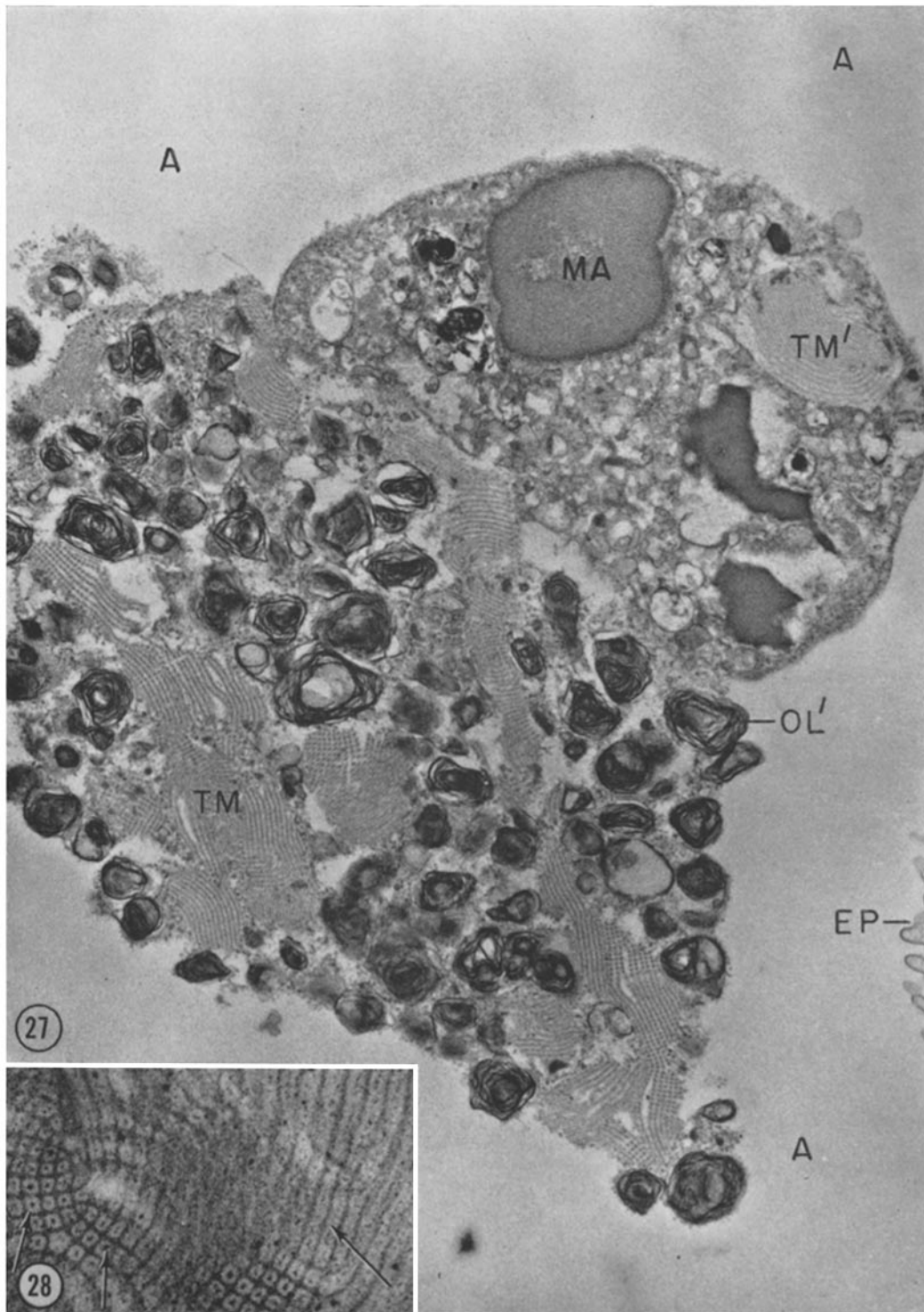
FIGURE 27   Mass of tubular myelin figures (*TM*) and lamellated osmiophilic spheroids (*OL'*) from alveolar exudate in lung after 72 hr exposure to oxygen. Macrophage (*MA*) is in process of phagocytosing this material (*TM'*). × 13,800.

FIGURE 28   Tubules of peculiar "myelin figures" are packed densely in square lattice and contain fine inner tubule or central filament (arrows), as shown in longitudinal and transverse sections. × 71,800.

for other organs (54) are difficult to correlate with the present pulmonary findings.

Specificity of Toxic Oxygen Effect

In various studies (55–57) the supplementary role of factors other than oxygen for the development of the oxygen toxicity syndrome is stressed. Among these, high pCO_2 levels appear to be most important; in the present experiments, CO_2 concentration was kept below 0.1% so that this factor can be excluded. Contaminants, particularly pulmonary irritants, were not found in the chamber atmosphere. Since the experiments were conducted at sea level pressure, no barometric effects must be assumed. Therefore it can be safely concluded that the effects observed are related to the high partial pressure of oxygen in the medium breathed. It may be interesting to mention, in this context, that the breathing of pure oxygen at $\frac{1}{3}$ atmosphere during a 2 wk period produced no similar morphologic changes in the lung tissue of identical rats (58).

The present experiments were conducted on nonpathogen-free, young Sprague-Dawley rats. It appears that sensitivity to elevated oxygen concentrations varies considerably among different species, as well as between strains of the same species (59, 60). Sprague-Dawley rats were selected for this study because of their rapid development of pulmonary changes. It also appears that pathogen-free animals are less susceptible than regular stocks (59, 60). This may indicate that oxygen alone cannot produce toxic effects but that additional (endogenous) factors play an essential role, a point to which reference will be made below.

Remarks on Possible Mechanism of Oxygen Effect on Cells

Breathing pure oxygen at 1 atm. ambient pressure causes severe damage to lung tissue and is found to gravely impair lung function. The change is progressive and eventually leads to asphyctic death. The present study has localized the primary injury in endothelial cells of alveolar capillaries

and has explained the other changes as its consequence. It would be tempting to speculate on the specific cytotoxic mechanisms involved in endothelial cell damage; inhibition of enzymes, formation of lipid peroxides, and other biochemical disturbances have been suggested as playing an eminent role (see reference 57). However, it is not possible to interpret conclusively our present data in terms of these biochemical findings.

The most puzzling observation relates to our finding that endothelial cells are damaged first by an agent that has to traverse a similar tissue layer before reaching its target. The question why epithelial cells, which are directly exposed to the high oxygen pressure, are not damaged, whereas endothelial cells undergo such early and drastic changes, remains unanswered. It may be proposed that oxygen can exert its cytotoxic effect only in the presence of additional factors; this is suggested from studies on enzyme inhibition by oxygen, which depends on contamination of the preparations by various compounds (see reference 57). If such factors are endogenous and can be supplied by the blood, endothelial cells of alveolar capillaries could be regarded as the site of most intense interaction between oxygen coming from alveolar air and "additional factors" supplied by capillary blood. This possibility is being investigated further.

BIBLIOGRAPHY

1. DONALD, K. W. 1947. Oxygen poisoning in man. *Brit. Med. J.* 1:688.
2. BECKER-FREYSENG, H., and H. G. CLAMANN. 1950. Physiological and patho-physiological effects of increased oxygen tension. *In* German Aviation Medicine in World War II. United States Government Printing Office, Washington, D.C. 1:493.

3. Mullinax, P. F., and D. E. Beischer. 1958. Oxygen toxicity in aviation medicine; a review. *J. Aviation Med.* 29:660.

4. Ernsting, J. 1960. Some effects of oxygen breathing. *Proc. Roy. Soc. Med.* 53:96.

5. Dubois, A. B. 1962. Oxygen toxicity. *Anaesthesiology.* 23:473.

6. Gerschman, R. 1962. The biological effects of increased oxygen tension. *In* Man's Dependence on the Earthly Atmosphere. K. E. Schaefer, editor. Macmillan Co., New York. 170.

7. Roth, E. M. 1964. Space Cabin Atmospheres, part I: Oxygen toxicity. NASA publication, NASA-SP-47, Washington, D.C.

8. Lambertsen, C. J. 1965. Effects of oxygen at high partial pressures. *In* Handbook of Physiology, Section 3: Respiration, W. O. Fenn and H. Rahn, editors. American Physiological Society Washington, D.C. 2:1027.

9. Smith, J. L. 1899. The pathological effects due to increase of oxygen tension in the air breathed. *J. Physiol.* 24:19.

10. Binger, C. A. L., J. M. Faulkner, and R. L. Moore. 1927. Oxygen poisoning in mammals. *J. Exptl. Med.* 45:849.

11. Becker-Freyseng, H., und H. G. Clamann. 1939. Zur Frage der Sauerstoffvergiftung. *Klin. Woschr.* 18:1385.

12. Clamann, H. G., H. Becker-Freyseng, und G. Liebegott. 1940. Das allgemeine Verhalten und die morphologischen Lungenveränderungen verschiedener Tierarten bei langer Einwirkung erhöhten Sauerstoffteildruckes. *Luftfahrtmedizin.* 5:17.

13. Pichotka, J. 1941. Ueber die histologischen Veränderungen der Lunge nach Atmung von hochkonzentriertem Sauerstoff im Experiment. *Beitr. Pathol. Anat. Allgem. Pathol.* 105:381.

14. Liebegott, G. 1941. Ueber Organveränderungen bei langer Einwirkung von Sauerstoff mit erhöhtem Partialdruck im Tierexperiment. *Beitr. Pathol. Anat. Allgem. Pathol.* 105:413.

15. Paine, J. R., D. Lynn, and A. Keys. 1941. Observations on the effect of the prolonged administration of high oxygen concentration to dogs. *J. Thorac. Surg.* 11:151.

16. Stadie, W. C., B. D. Riggs, and N. Haugaard. 1944. Oxygen poisoning. *Am. J. Med. Sci.* 207:84.

17. Bean, J. W. 1945. Effects of oxygen at increased pressure. *Physiol. Rev.* 25:1.

18. Ohlsson, W. T. L. 1947. A study on oxygen toxicity at atmospheric pressure. *Acta Med. Scand. Suppl.* 190:1.

19. Hemingway, A., and W. L. Williams. 1952. Pulmonary edema in oxygen poisoning. *Proc. Soc. Exptl. Biol. Med.* 80:331.

20. Penrod, K. E. 1956. Nature of pulmonary damage produced by high oxygen pressure. *J. Appl. Physiol.* 9:1.

21. Weir, F. W., D. W. Bath, P. Yevich, and F. W. Oberst. 1961. A study of the effects of continuous inhalation of high concentrations of oxygen at ambient pressure and temperature. NASA Technical Report ASD-TR-61-664. Washington, D.C.

22. Heppleston, A. G., and J. D. Simnett. 1964. The tissue reaction to hyperbaric oxygen. *Lancet.* 1:1135.

23. Cederberg, A., S. Hellsten, and G. Miörner. 1965. Oxygen treatment and hyaline pulmonary membranes in adults. *Acta Pathol. Microbiol. Scand.* 64:450.

24. Fuson, R. L., et al. 1965. Clinical hyperbaric oxygenation with severe oxygen toxicity: report of a case. *New Engl. J. Med.* 273(8):415.

25. Pratt P. C. 1958. Pulmonary capillary proliferation induced by oxygen inhalation. *Am. J. Pathol.* 34:1033.

26. Schulz, H. 1956. Ueber den Gestaltwandel der Mitochondrien im Alveolarepithel unter CO_2 und O_2 Atmung. *Naturwissenschaften.* 9:205.

27. Treciokas, L. J. 1959. The effect of "oxygen poisoning" on alveolar cell mitochondria as revealed by electron microscopy. *Aerospace Med.* 30(9):674.

28. Cedergren, B., Gyllensten, L., and Wersäll, J. 1959. Pulmonary damage caused by oxygen poisoning. *Acta Paediat.* 48:477.

29. Kistler, G. S., P. R. B. Caldwell, and E. R. Weibel. 1965. Electron Microscopic and morphometric study of rats exposed to 98.5% oxygen at atmospheric pressure. Aerospace Medical Research Laboratories, AMRL, Technical Report AMRL-TR-65-66.

30. Kistler, G. S., P. R. B. Caldwell, and E. R. Weibel.: Quantitative electron microscope studies of lung damage in rats breathing 98.5% oxygen at 765 Torr: A preliminary report. *In* Hyperbaric Medicine. I. W. Brown, Jr., editor. National Academy of Science–National Research Council Publication No. 1404. Washington, D. C. In press.

31. Felig, P., and W. L. Lee, Jr. 1965. Effects of sodium lactate on oxygen toxicity in the rat. *Ann. N.Y. Acad. Sci.* 121:829.

32. Caldwell, P. R. B., W. L. Lee, Jr., H. S. Schildkraut, and E. R. Archibald. 1966. Changes in lung volume, diffusing capacity and blood gases in men breathing oxygen. *J. Appl. Physiol.* 21:1477.

33. Luft, J. H. 1961. Improvements in epoxy-resin embedding methods. *J. Biophys. Biochem. Cytol.* 9:409.

34. Reynolds, E. S. 1963. The use of lead citrate at high pH as an electron opaque stain in electron microscopy. *J. Cell Biol.* 17:208.

35. Weibel, E. R. 1963. Morphometry of the Human Lung. Springer, Heidelberg, and Academic Press Inc., New York.

36. Weibel, E. R., G. S. Kistler, and W. F. Scherle. 1966. Practical stereological methods for morphometric cytology. *J. Cell Biol.* 30:23.

37. Weibel, E. R., and B. W. Knight. 1964. A morphometric study on the thickness of the pulmonary air-blood barrier. *J. Cell Biol.* 21: 367.

38. Van der Waerden, B. L. 1957. Mathematische Statistik. Springer, Berlin.

39. Linder, A. 1961. Statistische Methoden. Birkhäuser, Basel.

40. Low, F. N. 1953. The pulmonary alveolar epithelium of laboratory mammals and man. *Anat. Record.* 117:241.

41. Clemens, H. J. 1954. Elektronenmikroskopische Beobachtungen an der Lungenalveole. *Gegenbaurs Morphol. Jahrb.* 94:471.

42. Policard, A., A. Collet, and S. Pregermain. 1959. Recherches au microscope électronique sur les cellules pariétales alvéolaires du poumon des mammifères. *Z. Zellforsch.* 50:561.

43. Groniowski, J., and W. Djaczenko. 1960. The ultrastructure of rat lung in the pre- and postnatal period. *Intern. Kongr. Elektronenmikroskopie 4 Berlin 1958 Verhandl.* 2:404.

44. Rhodin, J. A. G. 1962. The diaphragm of capillary endothelial fenestrations. *J. Ultrastruct. Res.* 6:171.

45. Elfvin, L.-G. 1965. The ultrastructure of capillary fenestrae in the adrenal medulla of the rat. *J. Ultrastruct. Res.* 12:687.

46. Farquhar, M. G., and G. E. Palade. 1963. Junctional complexes in various epithelia. *J. Cell. Biol.* 17:375.

47. Campiche, M. 1960. Les inclusions lamellaires des cellules alvéolaires dans le poumon du raton. *J. Ultrastruct. Res.* 3:302.

48. Weibel, E. R., G. S. Kistler, and G. Töndury. 1966. A stereologic electron microscope study of "tubular myelin figures" in alveolar fluids of rat lungs. *Z. Zellforsch.* 69:418.

49. Leeson, T. S., and C. R. Leeson. 1966. Osmiophilic lamellated bodies and associated material in lung alveolar spaces. *J. Cell Biol.* 28:577.

50. Sun, C. N. 1966. Lattice structures and osmio-

philic bodies in the developing respiratory tissue of rats. *J. Ultrastruct. Res.* 15:380.

51. Cusick, P. L., O. O. Benson, and W. M. Boothby. 1940. Effect of anoxia and of high concentrations of oxygen on the retinal vessels. *Proc. Mayo Clin.* 15:500.

52. Asthon, N., B. Ward, and G. Serpell. 1954. Effect of oxygen on developing retinal vessels with particular reference to the problem of retrolental fibroplasia. *Brit. J. Ophthalmol.* 38:397.

53. Patz, A., A. Eastham, D. H. Higginbotham, and T. Kleh. 1953. Oxygen studies in retrolental fibroplasia. *Am. J. Ophthalmol.* 36:1511.

54. Schaffner, F., and P. Felig. 1965. Changes in hepatic structure in rats produced by breathing pure oxygen. *J. Cell Biol.* 27(3):505.

55. Campbell, J. A. 1938. Effects of oxygen pressure as influenced by external temperature, hormones and drugs. *J. Physiol.* 92:29.

56. Taylor, D. W. 1956. The effects of Vitamin E and of methylene blue on the manifestations of oxygen poisoning in the rat. *J. Physiol.* 131:200.

57. Davies, H. C., and R. E. Davies. 1965. Biochemical aspects of oxygen poisoning. *In* Handbook of Physiology, Section 3: Respiration. W. O. Fenn, and H. Rahn, editors. American Physiological Society, Washington. 2:1047.

58. Kistler, G. S., P. R. B. Caldwell, and E. R. Weibel. 1966. Electron microscopic and Morphometric study of rat Lungs Exposed to 97% Oxygen at 258 torr (27,000 feet). Aerospace Medical Research Laboratories, AMRL, Annual Summary Report No. II. 1966.

59. Back, K. C. 1966. Toxicity studies on animals exposed continuously for periods up to 235 days to a 5 psia 100% oxygen atmosphere. *In* Proceedings of the 2nd Annual Conference on Atmospheric Contamination in Confined Spaces. A. A. Thomas, editor. Aerospace Medical Research Laboratories. 6570th AMRL, Wright-Patterson AFB, Ohio. In press.

60. Robinson, F. R. 1966. Pathological evaluation of oxygen toxicity at near-ambient pressures. *In* Proceedings of the 2nd Annual Conference on Atmospheric Contamination in Confined Spaces. A. A. Thomas, editor. Aerospace Medical Research Laboratories. 6570th AMRL, Wright-Patterson, AFB, Ohio, In press.